Recent developments in understanding short-range correlations

Axel Schmidt

MIT

April 13, 2019

Short-range correlations produce a complicated picture.

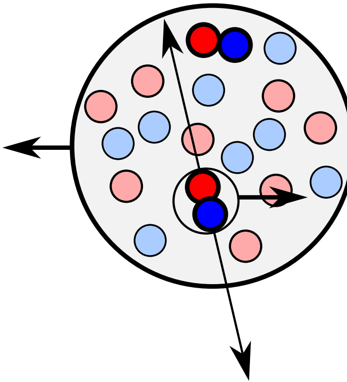

The short-distance part of the *NN*-interaction is not well-constrained by data.

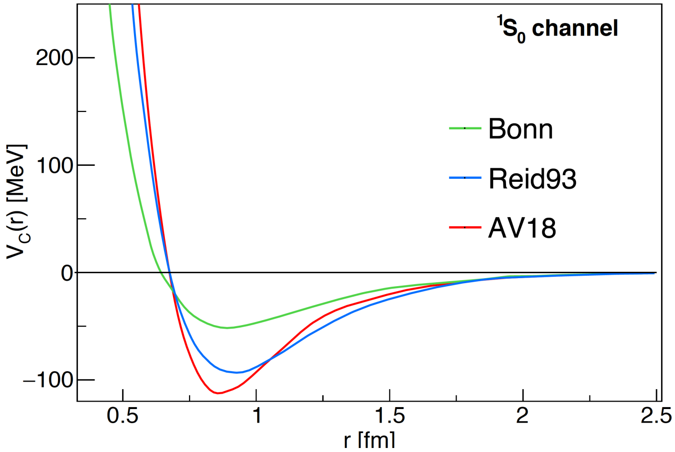

Figure courtesy of Reynier Cruz-Torres

Short-range correlations produce a complicated picture.

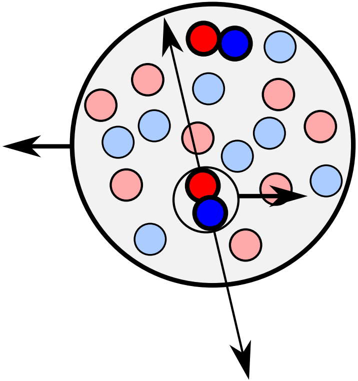

We now have a consistent scale-separated view of SRCs.

Three important properties:

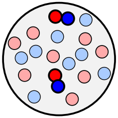

Pair abundances

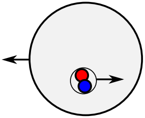

Pair CM motion

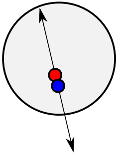

Pair relative motion

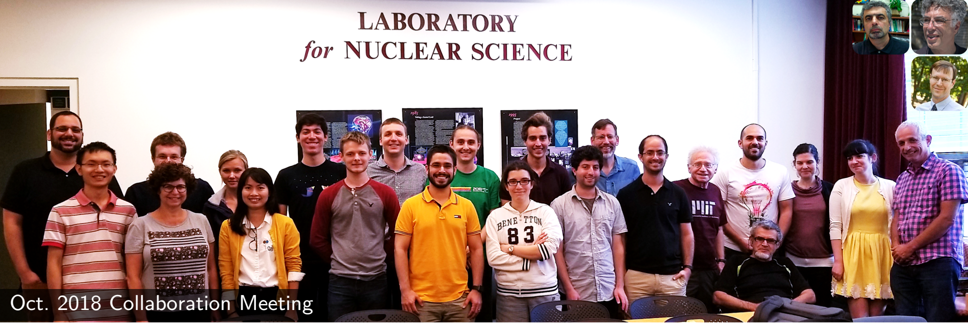

Oct. 2018 Collaboration Meeting

2018/19 Publications*

Exp:

- Nature 566, 354 (2019)
- Nature, 560, 617 (2018)
- PRL, In-Print (2019)
- PRL 121, 092501 (2018)

arXiv: 1811.01823 (accepted to PRL)
1902.06358 (\w PRL)

Theory:

- Physics Letters B 791, 242 (2019)
- Physics Letters B 785, 304 (2018)
- Physics Letters B 780, 211 (2018)
- CPC 42, 064105 (2018)

arXiv: 1812.08051 (\w PLB)
1805.12099 (\w PLB)

*Just by us. More by others…

In my talk today:

1. Generalized Contact Formalism
   - Scale-separated description of SRCs
2. Moving from GCF to cross sections
   - Modeling abundances, CM motion, relative motion
3. Comparisons to data
   - Constraining the short-range *NN* interaction

We have lots of data to compare to!

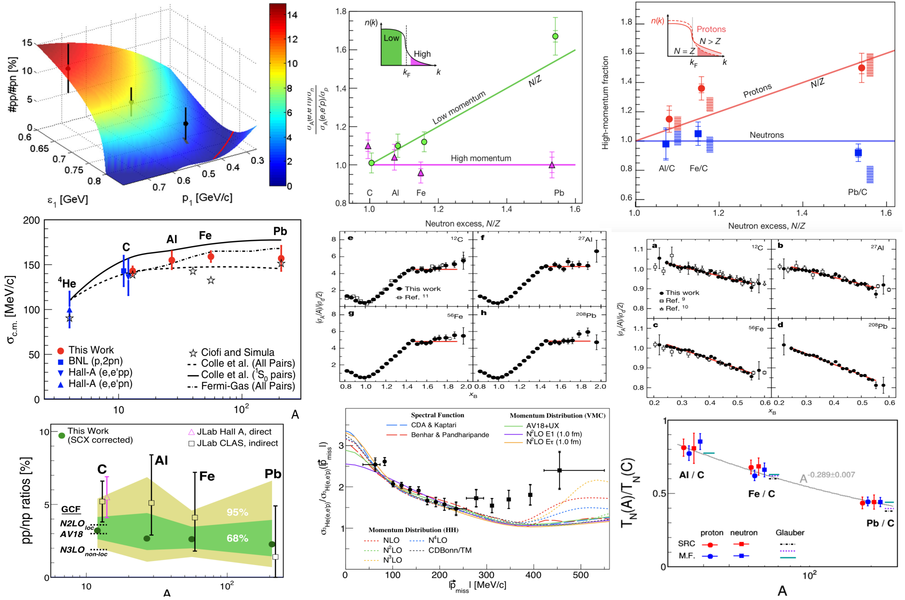

Generalized Contact Formalism exploits scale separation.

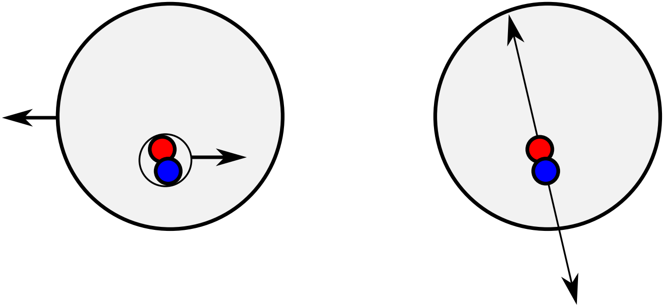

$$P_{CM} \quad \ll \quad p_{rel.}$$

R. Weiss, R. Cruz-Torres et al., PLB 780 211–215 (2018)

Generalized Contact Formalism exploits scale separation.

When two particles are in close proximity:

$$\Psi(r_{ij} \to 0) \longrightarrow \varphi^{\alpha}(r_{ij}) \times A(R_{ij}, \vec{r}_{k \neq i,j})$$

Generalized Contact Formalism exploits scale separation.

When two particles are in close proximity:

$$\Psi(r_{ij} \to 0) \longrightarrow \varphi^{\alpha}(r_{ij}) \times A(R_{ij}, \vec{r}_{k \neq i,j})$$

$$\rho_2(r_{ij}) \longrightarrow \sum_{\alpha} C_{\alpha} |\varphi^{\alpha}(r_{ij})|^2$$

Generalized Contact Formalism exploits scale separation.

When two particles are in close proximity:

$$\Psi(r_{ij} \to 0) \longrightarrow \varphi^{\alpha}(r_{ij}) \times A(R_{ij}, \vec{r}_{k \neq i,j})$$

$$\rho_2(r_{ij}) \longrightarrow \sum_{\alpha} C_{\alpha} |\varphi^{\alpha}(r_{ij})|^2$$

When two particles have high relative momentum:

$$\tilde{\rho}_2(k_{ij}) \longrightarrow \sum_{\alpha} C_{\alpha} |\tilde{\varphi}^{\alpha}(k_{ij})|^2$$

Universal φ^{α} functions are Schrödinger solutions for a given NN potential.

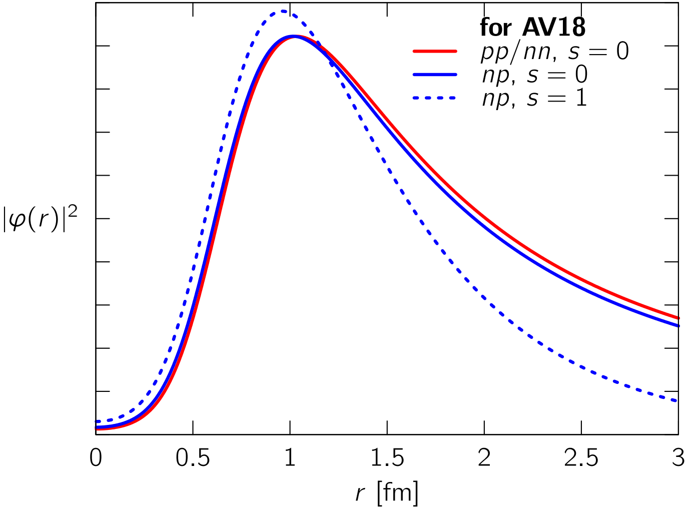

Universal φ^α functions are Schrödinger solutions for a given NN potential.

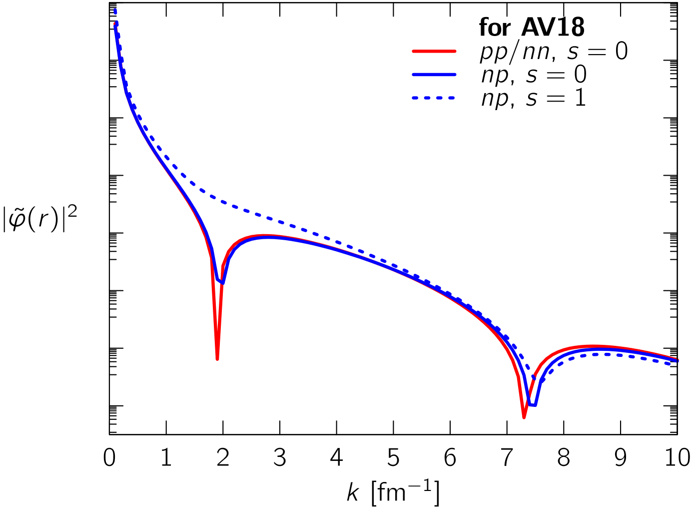

Generalized Contact Formalism exploits scale separation.

When two particles are in close proximity:

$$\rho_2(r_{ij}) \longrightarrow \sum_\alpha C_\alpha |\varphi^\alpha(r_{ij})|^2 \ \checkmark$$

When two particles have high relative momentum:

$$\tilde{\rho}_2(k_{ij}) \longrightarrow \sum_\alpha C_\alpha |\tilde{\varphi}^\alpha(k_{ij})|^2 \ \checkmark$$

Contacts can be determined from fits to ab initio calculations.

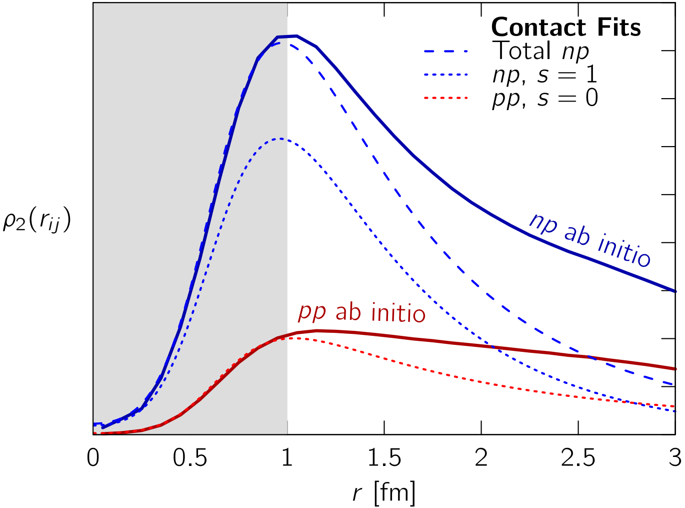

These fits faithfully reproduce high-momentum tails.

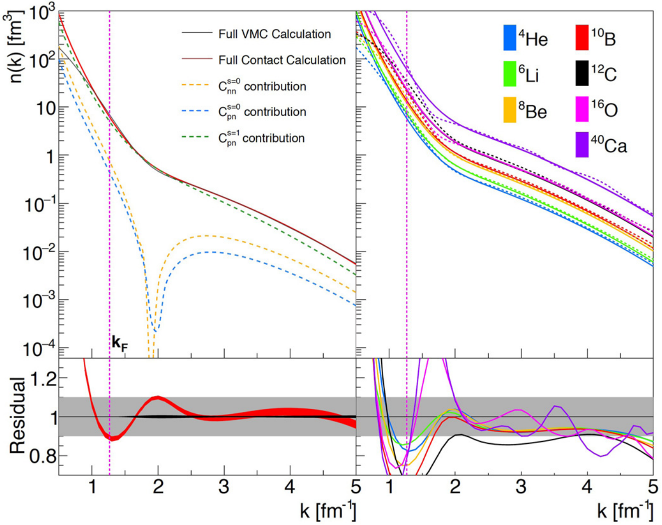

. . . and short-distance two-body densities.

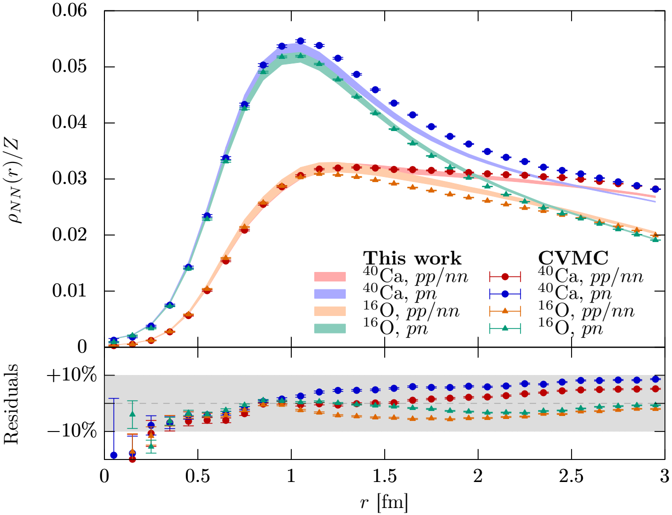

R. Cruz-Torres, **A. Schmidt** et al., PLB 785 p.304 (2018)

Different *NN* interactions can lead to very different two-body densities.

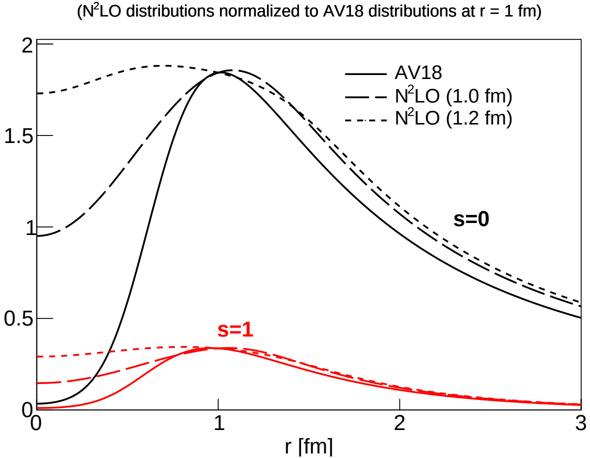

Figure courtesy of Reynier Cruz-Torres

Different *NN* interactions can lead to very different two-body densities.

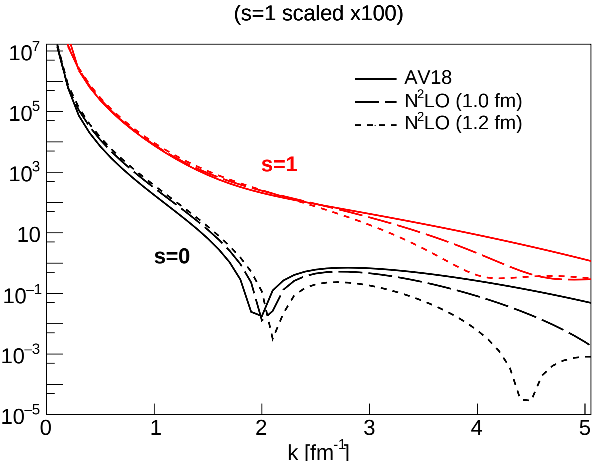

Figure courtesy of Reynier Cruz-Torres

Relative SRC pair abundances are largely scale and scheme independent.

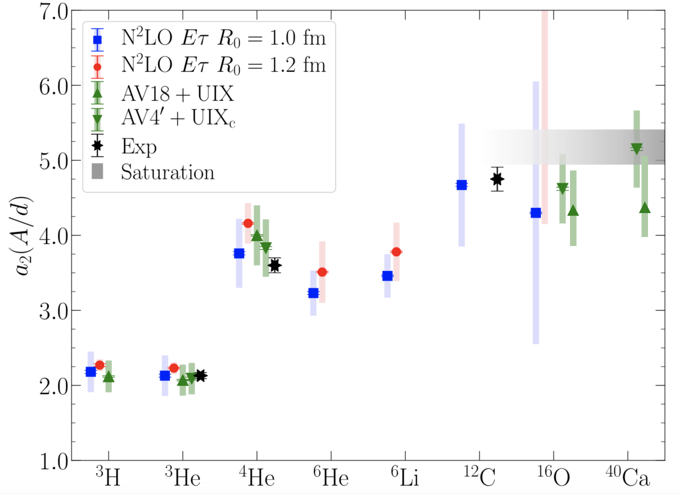

Adapted from J. Lynn et al., arXiv:12587 (2019)

We can use GCF to calculate this plane-wave reaction.

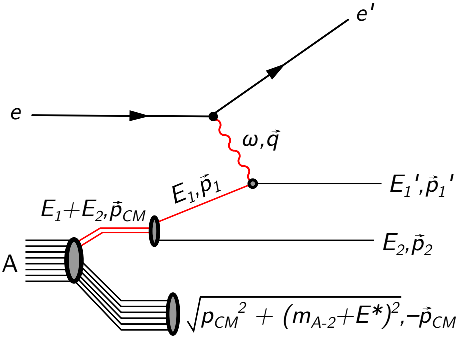

We can use GCF to calculate this plane-wave reaction.

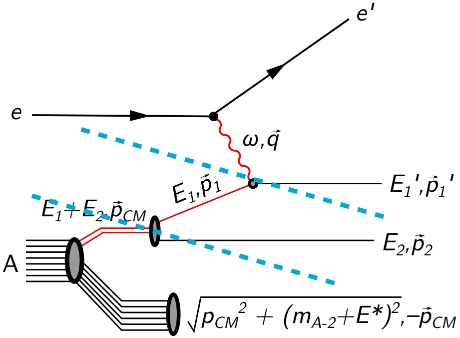

$$p_{CM} \ll p_{rel} \ll q$$

GCF allows us to calculate a spectral function or a decay function.

R. Weiss et al., PLB 790 p 241 (2019)

Two-nucleon knockout:

$$D(E_1, p_1, p_2) = \sum_\alpha C_\alpha |\varphi^\alpha(p_{rel})|^2 n(p_{CM}) \delta(E_i - E_f)$$

GCF allows us to calculate a spectral function or a decay function.

R. Weiss et al., PLB 790 p 241 (2019)

Two-nucleon knockout:

$$D(E_1, p_1, p_2) = \sum_\alpha C_\alpha |\varphi^\alpha(p_{rel})|^2 n(p_{CM}) \delta(E_i - E_f)$$

Single-nucleon knockout:

$$S(E_1, p_1) = \sum_\alpha C_\alpha \int \frac{d^3\vec{p}_2}{(2\pi)^3} |\varphi^\alpha(p_{rel})|^2 n(p_{CM}) \delta(E_i - E_f)$$

GCF allows us to calculate a spectral function or a decay function.

R. Weiss et al., PLB 790 p 241 (2019)

Two-nucleon knockout:

$$D(E_1, p_1, p_2) = \sum_\alpha C_\alpha |\varphi^\alpha(p_{rel})|^2 n(p_{CM}) \delta(E_i - E_f)$$

Single-nucleon knockout:

$$S(E_1, p_1) = \sum_\alpha C_\alpha \int \frac{d^3\vec{p}_2}{(2\pi)^3} |\varphi^\alpha(p_{rel})|^2 n(p_{CM}) \delta(E_i - E_f)$$

$$d\sigma \propto \sigma_{eN} \cdot S(E_1, p_1)$$

Ingredients to the GCF cross section

- Relative momentum $\longrightarrow$ *NN* interaction
- SRC pair abundances $\longrightarrow$ estimate from ab initio calcs.
- Pair center-of-mass motion

We measured the CM momentum distribution and confirmed its width is small.

E.O. Cohen et al., PRL 121 092501 (2018)

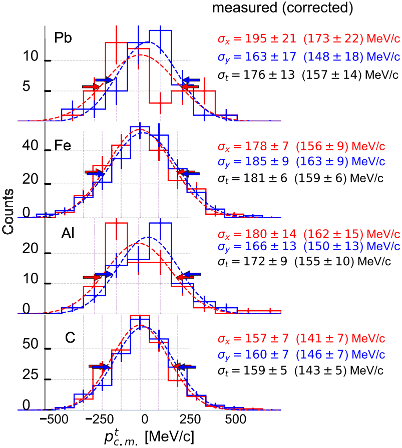

We measured the CM momentum distribution and confirmed its width is small.

E.O. Cohen et al., PRL 121 092501 (2018)

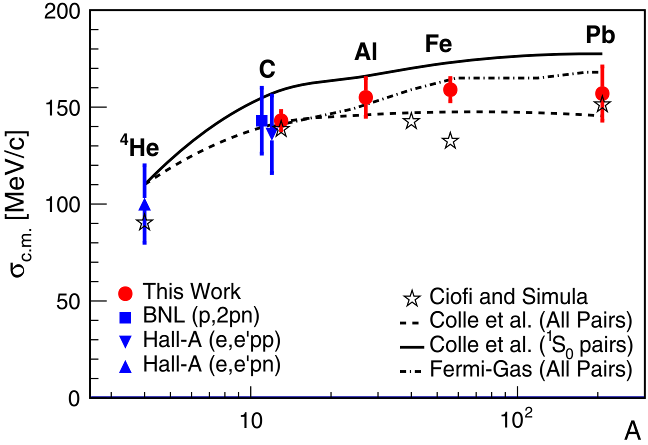

We can compare to data from the CLAS EG2 experiment.

- 5 GeV e^- beam
- C, Al, Fe, Pb
- CLAS detector

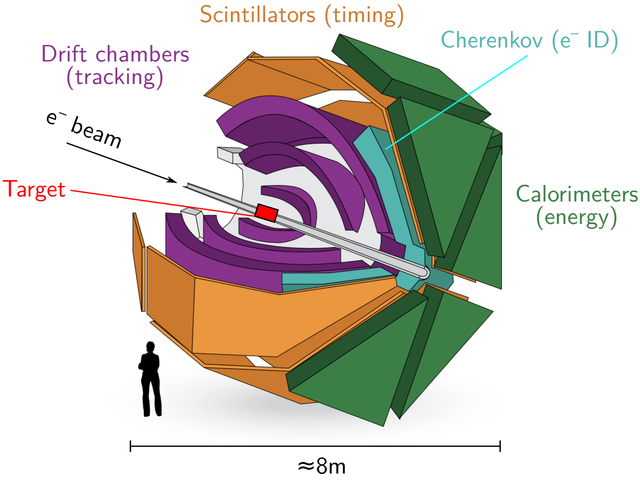

CLAS's large-acceptance is crucial for detecting multi-particle final states.

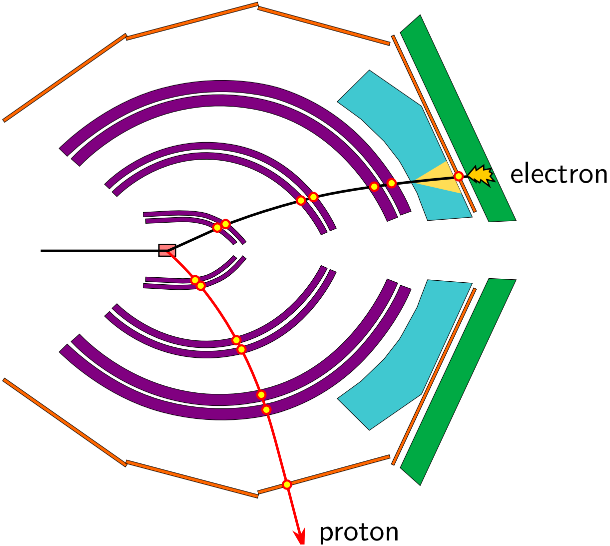

CLAS's large-acceptance is crucial for detecting multi-particle final states.

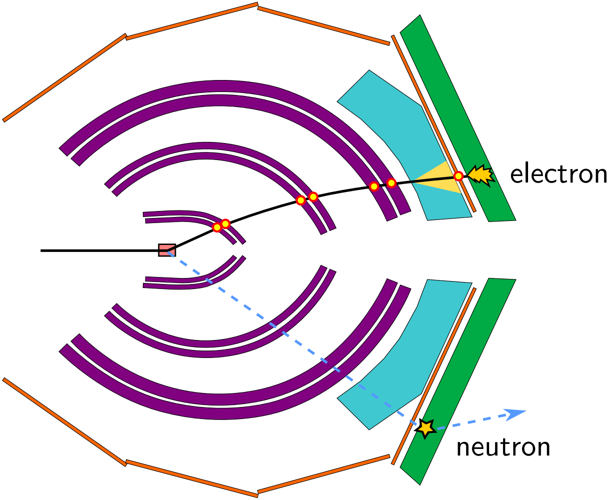

We've selected events to minimize competing reactions.

Isobar Config.

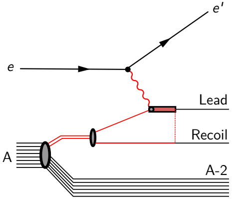

Meson-exchange curr.

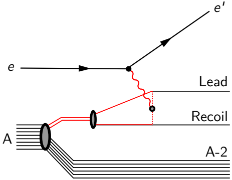

FSI within pair

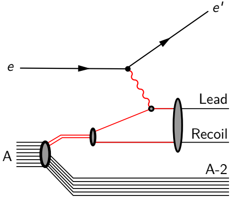

FSI with nucleus

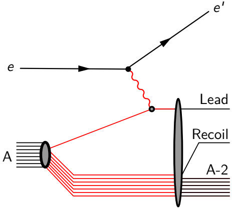

We've selected events to minimize competing reactions.

Isobar Config.

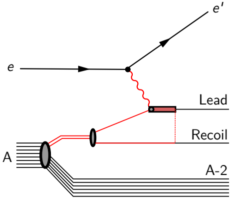

Meson-exchange curr.

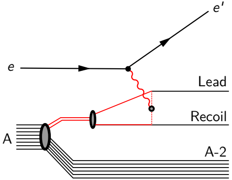

- $x_B > 1.2$
- High Q^2

FSI within pair

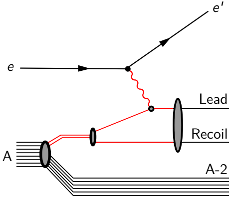

FSI with nucleus

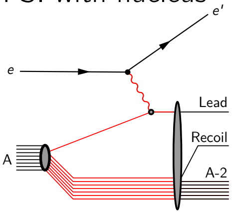

We've selected events to minimize competing reactions.

Isobar Config.

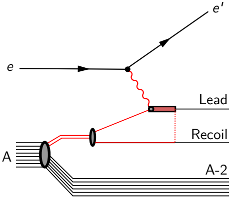

Meson-exchange curr.

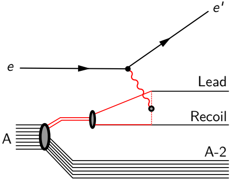

- $x_B > 1.2$
- High Q^2

FSI within pair

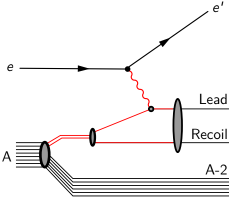

FSI with nucleus

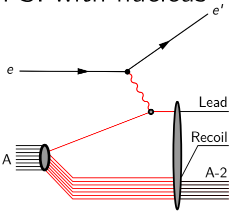

- Anti-parallel kinematics

SRC events are selected in kinematics that minimize final-state interactions.

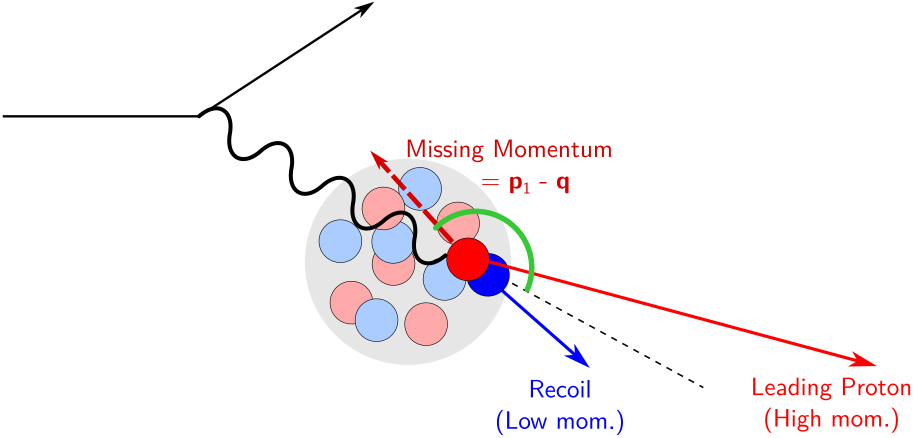

$\vec{p}_{\text{miss}}$ is anti-parallel to $\vec{q}$ for C, Al, Fe, Pb.

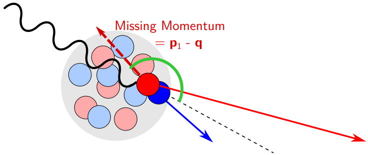

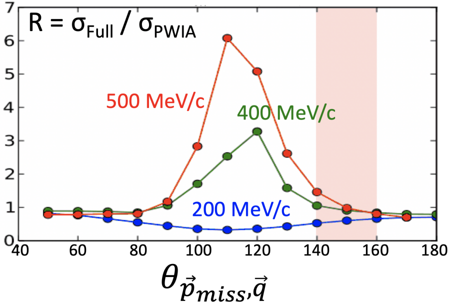

Figure courtesy of M. Sargsian

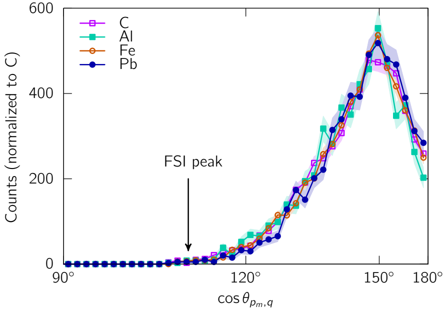

We remain anti-parallel over our p_{miss} range.

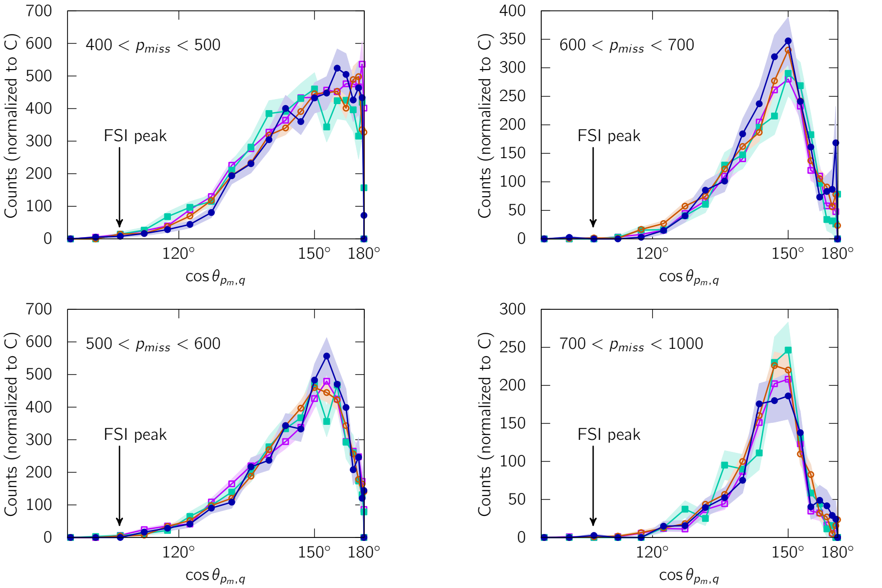

Connecting the model to data

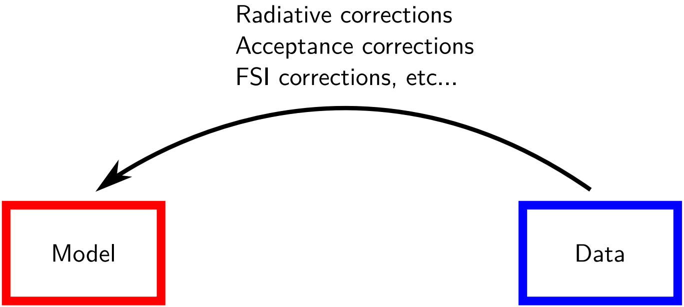

Connecting the model to data

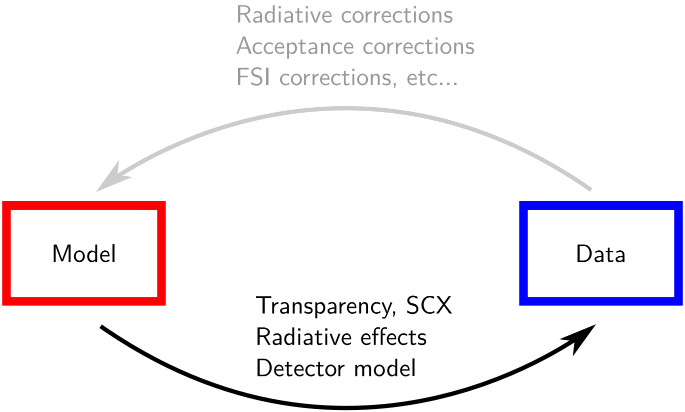

We forward propagate the model to the data.

1. Generate events according to model

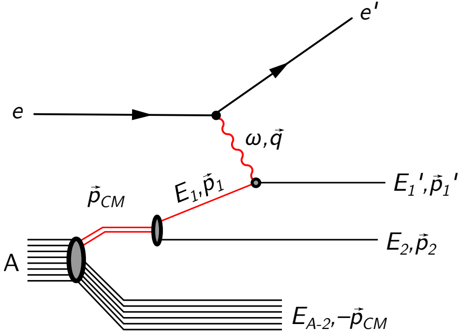

We forward propagate the model to the data.

1. Generate events according to model
2. Radiative effects

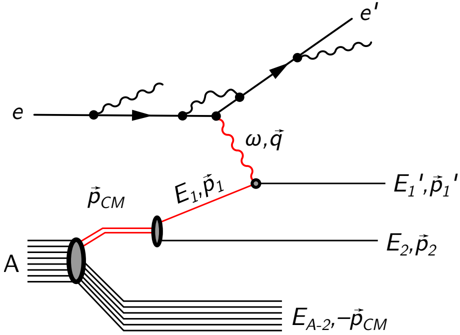

We forward propagate the model to the data.

1. Generate events according to model
2. Radiative effects
3. Transparency/SCX using Glauber

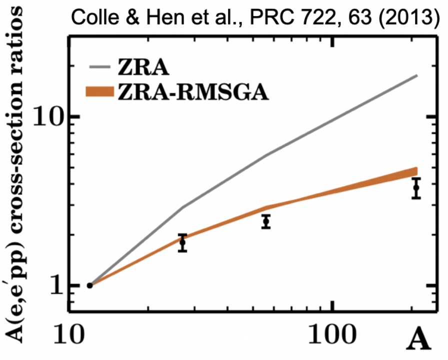

We forward propagate the model to the data.

1. Generate events according to model
2. Radiative effects
3. Transparency/SCX using Glauber
4. Detector acceptance

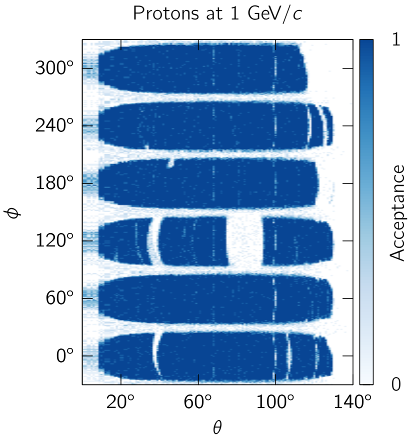

We forward propagate the model to the data.

1. Generate events according to model
2. Radiative effects
3. Transparency/SCX using Glauber
4. Detector acceptance
5. Same event selection as data

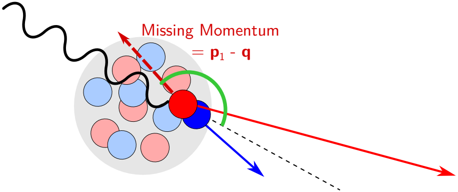

We compare our GCF calculation to several reactions.

- $^{12}\mathrm{C}(e, e'np)$
  - $0.4 < p_{miss} < 1.0 \quad \mathrm{GeV}/c$
  - Only a few dozen neutron events
  - arXiv:1810.05343, just accepted to PRL

- $^{12}\mathrm{C}(e, e'p)$ and $^{12}\mathrm{C}(e, e'pp)$
  - $0.4 < p_{miss} < 1.0 \quad \mathrm{GeV}/c$
  - Few hundred to few thousand events
  - Analysis under review (still preliminary!)

$^{12}C(e, e'pp)/^{12}C(e, e'np)$

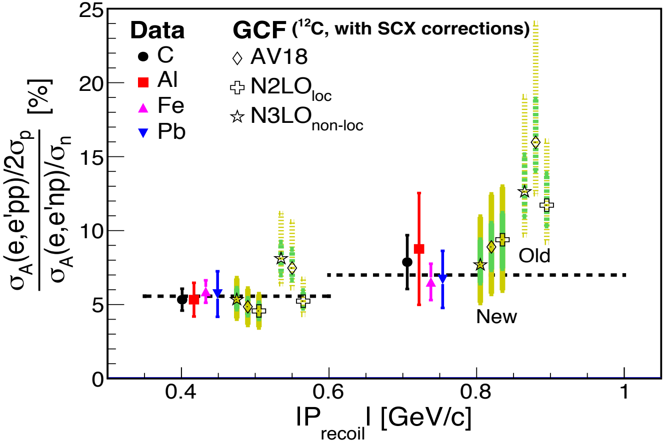

M. Duer, **A. Schmidt** et al., accepted to PRL (2019)

Comparison to $^{12}\mathrm{C}(e, e'p)$ and $^{12}\mathrm{C}(e, e'pp)$

- Carbon data only
  - Contacts determined from fits to ab initio VMC

Comparison to ^{12}C$(e, e'p)$ and ^{12}C$(e, e'pp)$

- Carbon data only
  - Contacts determined from fits to ab initio VMC
- *NN* interactions
  - AV18
  - Local χPT N2LO (1 fm cut-off)

Comparison to ^{12}C$(e, e'p)$ and ^{12}C$(e, e'pp)$

- Carbon data only
  - Contacts determined from fits to ab initio VMC
- *NN* interactions
  - AV18
  - Local χPT N2LO (1 fm cut-off)
- Model uncertainty from:

- Contacts
- σ_{CM}
- SCX prob.
- Transparency
- $A-2$ excitation E^*
- $p_{\text{rel.}}$ cut-off
- e^- res.
- p res.

The model accurately predicts kinematics.

$C(e, e'p)$ $C(e, e'pp)$

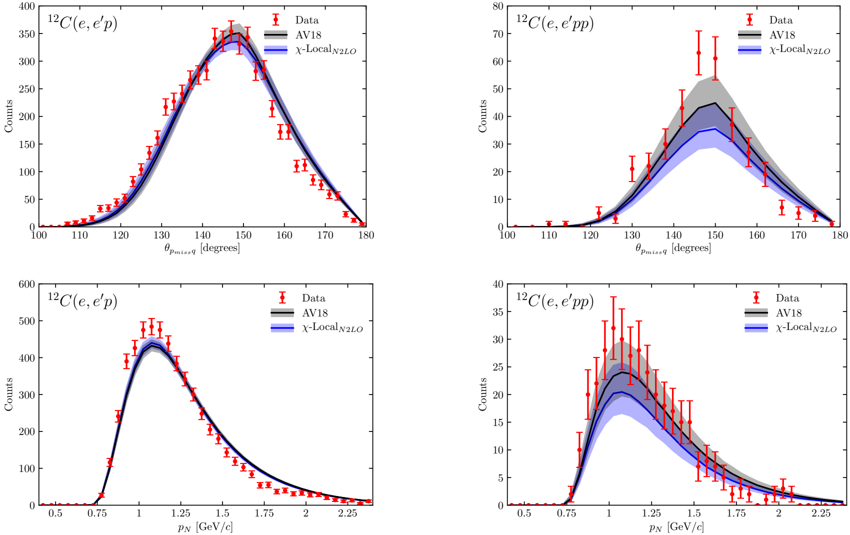

Missing momentum distributions show sensitivity to the *NN* interaction.

C$(e, e'p)$

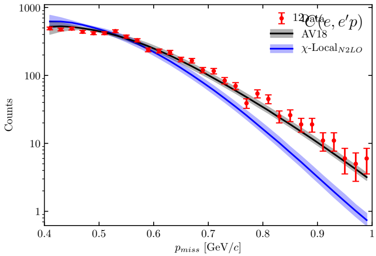

C$(e, e'pp)$

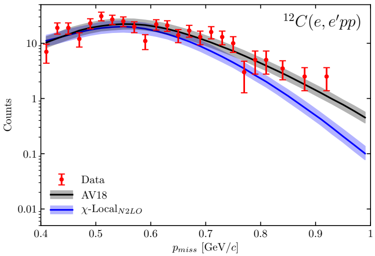

We can verify no significant FSIs.

- Different p_{miss} dependence for $e'p$, $e'pp$ events

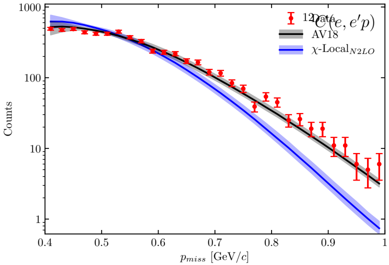

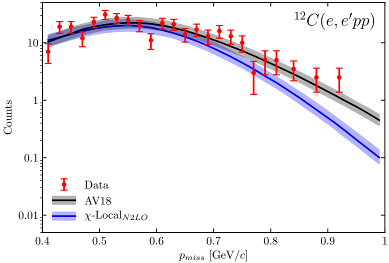

We can verify no significant FSIs.

- Different p_{miss} dependence for $e'p$, $e'pp$ events
- No excess transverse missing momentum

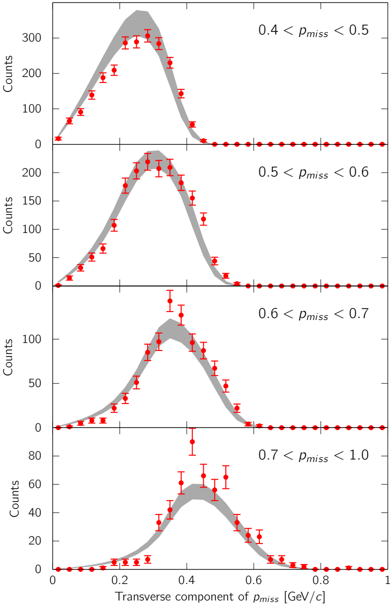

We can verify no significant FSIs.

- Different p_{miss} dependence for $e'p$, $e'pp$ events
- No excess transverse missing momentum
- No A-dependence in distributions!

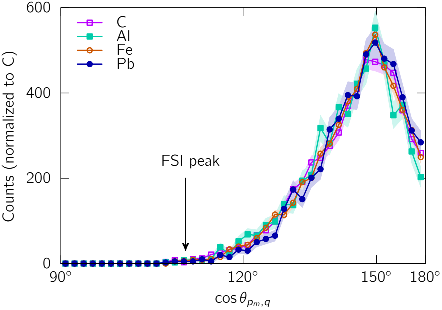

Missing-momentum and missing-energy

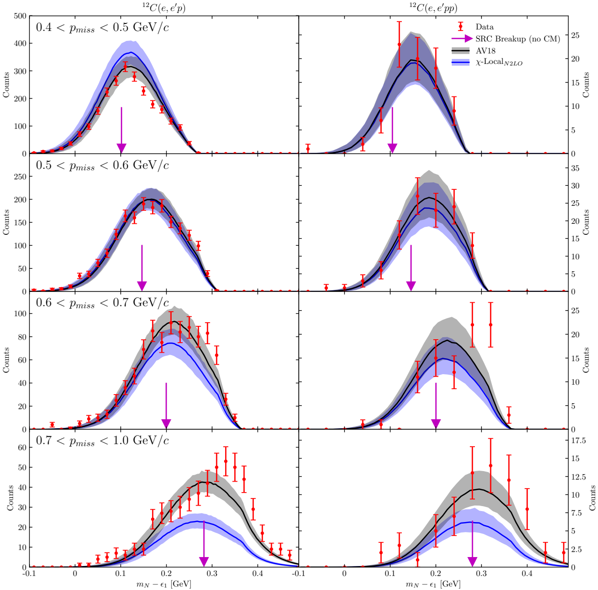

$(e, e'pp)/(e, e'p)$ ratio

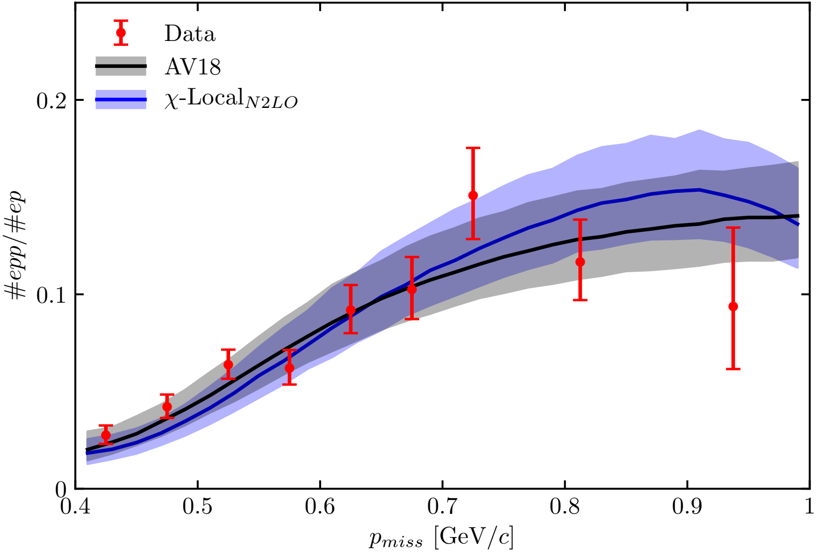

Isospin-dependence of the repulsive core

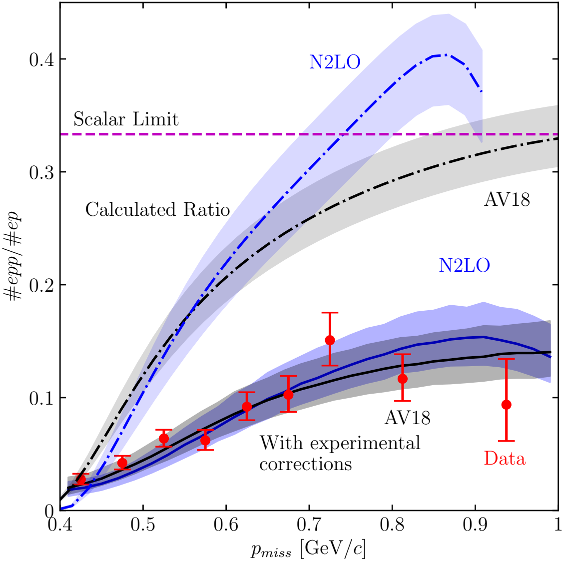

To recap:

1. Generalized Contact Formalism

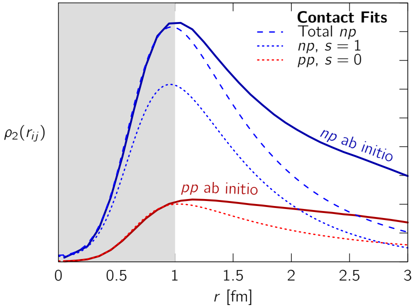

To recap:

1. Generalized Contact Formalism
2. GCF cross sections

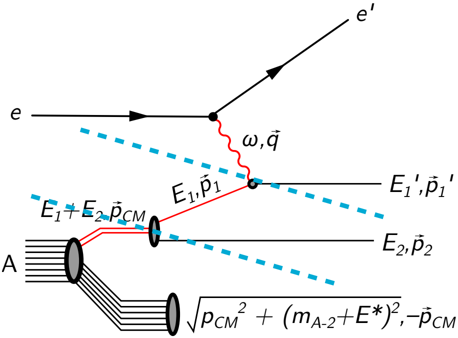

To recap:

1. Generalized Contact Formalism
2. GCF cross sections
3. Comparisons to data

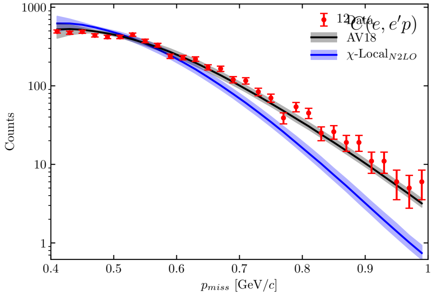

SRC data can constrain the *NN* interaction up to 1 GeV/*c*!

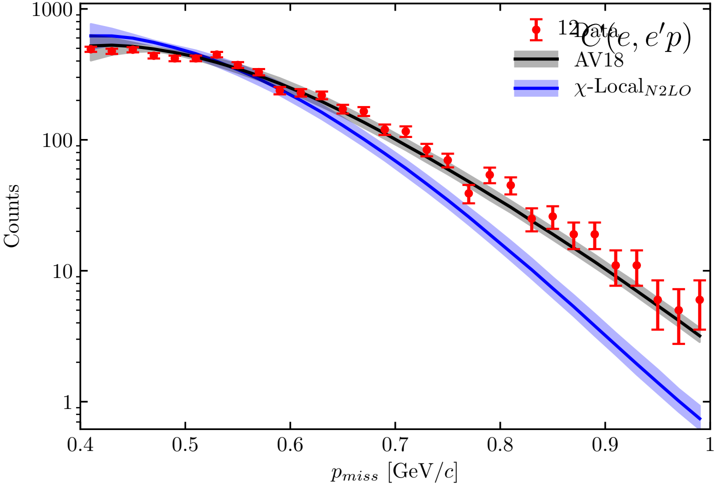

Different observables have different scale and scheme dependence.

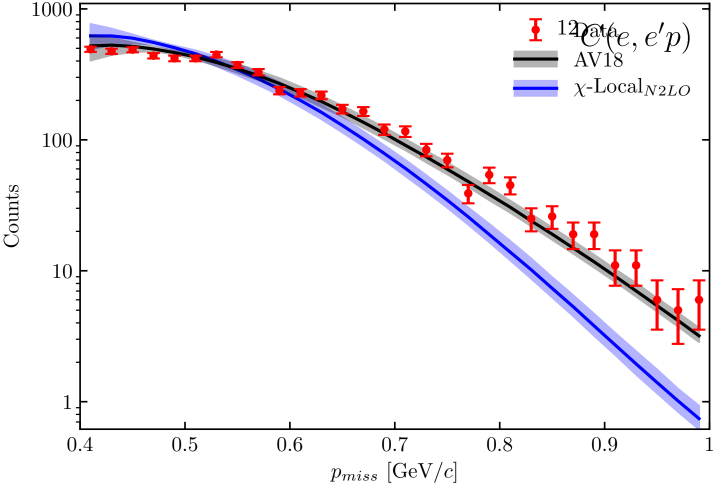

Different observables have different scale and scheme dependence.

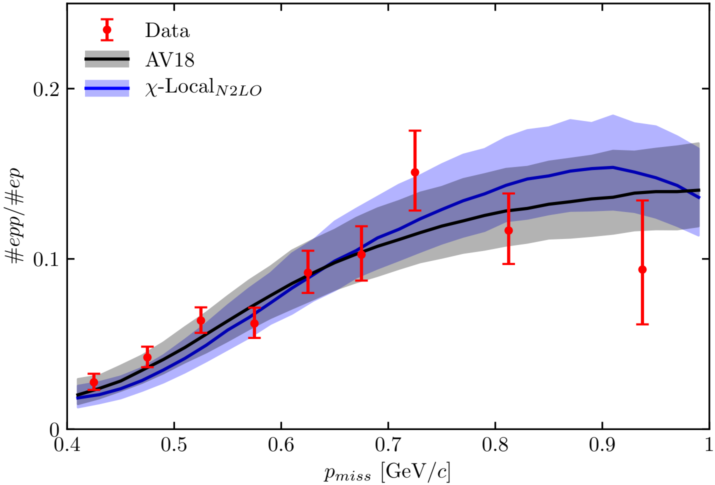

Different observables have different scale and scheme dependence.

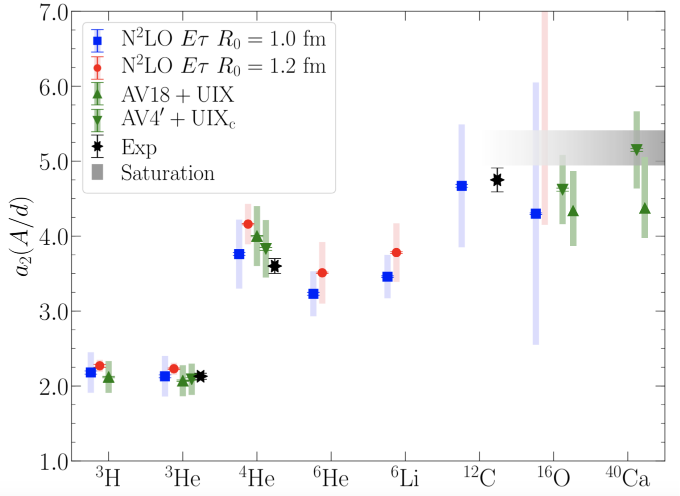

We now have a consistent scale-separated view of SRCs.

Three important properties:

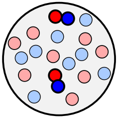

Pair abundances

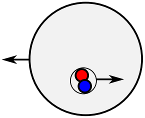

Pair CM motion

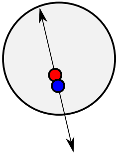

Pair relative motion

Other talks at this meeting:

In this session:
Or Hen

Later today:
Dien Nguyen (D15)

Sunday Morning:
Rey Cruz-Torres (G05)
Florian Hauenstein (H15)
Holly Szumila-Vance (H15)

Sunday Afternoon:
Afroditi Papadopoulou (J12)
Eli Piasetzky (L05)
Holly Szumila-Vance (L05)

Monday:
Holly Szumila-Vance (S01)

BACK-UP

Model cross section

$$\frac{d^8\sigma}{dQ^2 dx_B d\phi_e d^3\vec{p}_{CM} d\Omega_2} = \frac{\sigma_{eN}}{32\pi^4} n(\vec{p}_{CM}) \mathcal{J} \sum_\alpha C_\alpha |\tilde{\varphi}^\alpha(|\vec{p}_{rel}|)|^2$$

$$\mathcal{J} = \frac{E_1' E_2 p_2^2}{|E_2(p_2 - Z\cos\theta_{Z,2}) + E_1' p_2|} \frac{\omega}{2E_{beam} E_e x_B}$$

$$\vec{Z} \equiv \vec{q} + \vec{p}_{CM}$$

Leading and recoil protons are distinct.

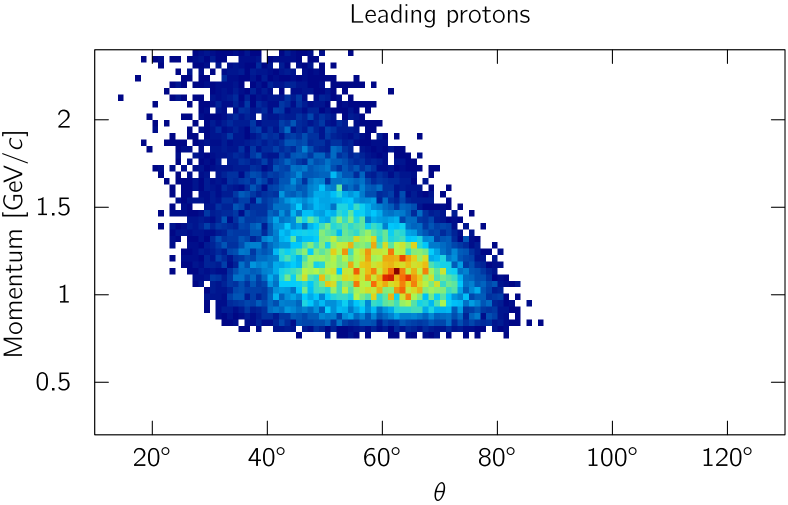

Leading and recoil protons are distinct.

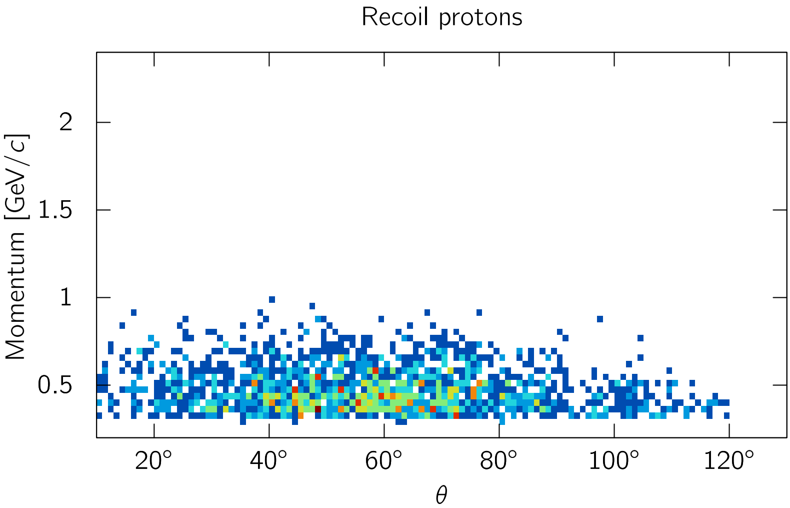

Leading and recoil protons are distinct.

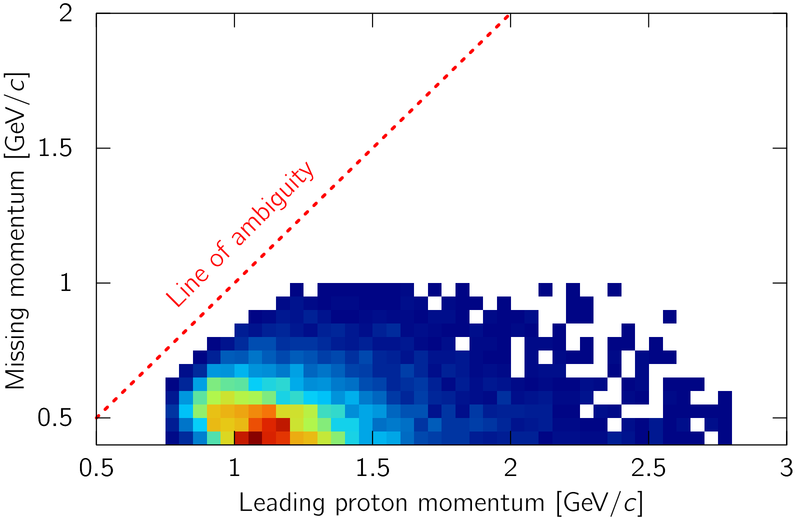

Missing momentum distributions show sensitivity to the *NN* interaction.

C$(e, e'p)$

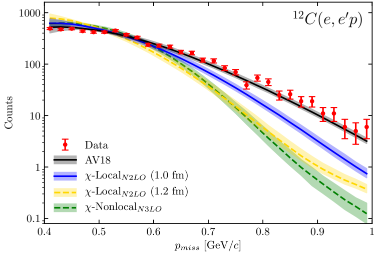

C$(e, e'pp)$

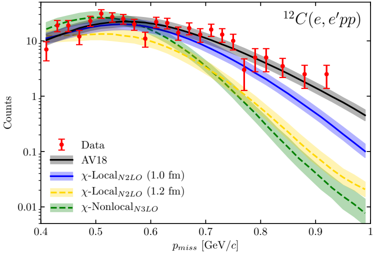

Implementation of single charge exchange (SCX) and transparency

Colle, Cosyn, Ryckebusch, PRC 034608 (2016)

Glauber calc of avg. probabilities:

- Leading $p \leftrightarrow n$
- Recoil $p \leftrightarrow n$
- Transparency factor for NN
- Transparency factor for N

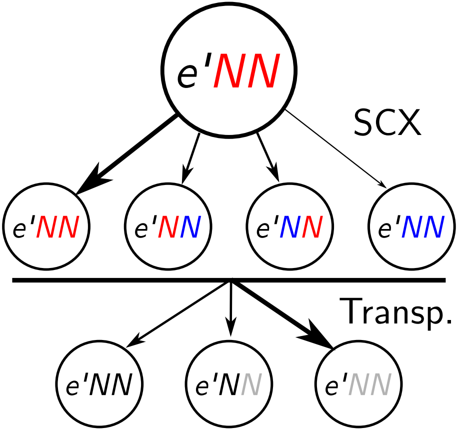

Inclusive scaling relies on kinematical assumptions.

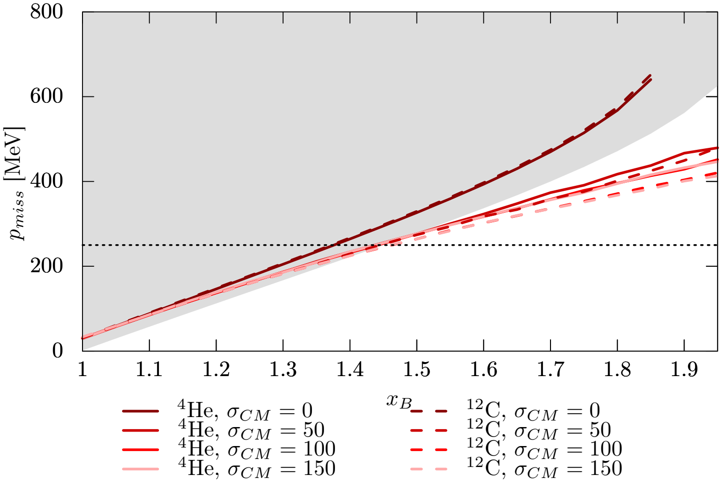

Inclusive scaling relies on kinematical assumptions.